Cell Adhesion & Migration 7:4, 370–376; July/August 2013; © 2013 Landes Bioscience

Abnormal myelination in the spinal cord of PTPα-knockout mice

Quan-Hong Ma[1,3,†], Tao Xiang[1,2,†], Zara Zhuyun Yang[1,2], Xu Zhang[1,2], Jude Taylor[1,2], and Zhi-Cheng Xiao[1,2,*]

[1]The Key Laboratory of Stem Cell and Regenerative Medicine; Institute of Molecular and Clinical Medicine; Kunming Medical College; Kunming, P.R. China; [2]Department of Anatomy and Developmental Biology; Monash University; Clayton, Melbourne, Australia; [3]Institute of Neuroscience; Soochow University; Suzhou, P.R. China

[†]These authors contributed equally to this work.

Keywords: PTPα, Myelination, Axon, Caspr, F3/contactin

PTPα interacts with F3/contactin to form a membrane-spanning co-receptor complex to transduce extracellular signals to Fyn tyrosine kinase. As both F3 and Fyn regulate myelination, we investigated a role for PTPα in this process. Here, we report that both oligodendrocytes and neurons express PTPα that evenly distributes along myelinated axons of the spinal cord. The ablation of PTPα in vivo leads to early formation of transverse bands that are mainly constituted by F3 and Caspr along the axoglial interface. Notably, PTPα deficiency facilitates abnormal myelination and pronouncedly increases the number of non-landed oligodendrocyte loops at shortened paranodes in the spinal cord. Small axons, which are normally less myelinated, have thick myelin sheaths in the spinal cord of PTPα-null animals. Thus, PTPα may be involved in the formation of axoglial junctions and ensheathment in small axons during myelination of the spinal cord.

Introduction

Myelinated axons can be divided into several domains: the nodes of Ranvier; the adjacent paranodes where terminal spiral oligodendroglial loops land; juxtaparanodes that are adjacent to the paranodes; and internodes that are located between the juxtaparanodes and wrapped by the compact layers of the myelin sheath. Notably, the paranodal region is an important domain for axoglial interactions. Well-defined, electron-dense, ladder-like partitions or septa, also called transverse bands, can be visualized at regular intervals in the narrow cleft between paranodal loops and the axolemma.[1,2] This structure also serves as a partial diffusion barrier to the periaxonal space to prevent the random lateral diffusion of membrane components.[3] Increasing evidence demonstrate that axoglial interactions at the paranodes regulate myelination. For instance, F3/contactin, a GPI-linked cell adhesion molecule of the immunoglobulin superfamily, interacts with the contactin-associated protein (Caspr) to constitute the transverse band at the paranode, which is a hallmark of the mature paranodal junction.[4] Our previous study has revealed that F3 promotes oligodendroglial maturation via the Notch/Deltex1 pathway through axoglial interaction.[5] However, the molecular mechanisms of paranodal formation are not fully understood.

The receptor protein tryrosine phosphatase α (PTPα) comprises an extracellular domain and an intracellular region containing two tandem catalytic domains.[6] PTPα interacts with F3 to form a *cis* membrane-spanning co-receptor complex, which potentially transduces extracellular signals to the tyrosine kinase Fyn.[7] Given that F3 is located at paranodes and promotes oligodendrocyte maturation as well as acts as a binding partner of PTPα, and that Fyn is implicated in oligodendrocyte differentiation and myelination,[8-10] we hypothesized that PTPα might be involved in modulating paranodal formation and myelination during CNS development. In this study, we found that PTPα was mainly expressed in both neurons and oligodendrocytes. In the spinal cord of PTPα-deficient mice, the formation of transverse bands at paranodal regions and myelination were advanced during early development. Notably, abnormal myelination was observed in the spinal cord of the adult mutant animals. These findings reveal that PTPα plays a role in myelination during the spinal cord development.

Results

PTPα is mainly expressed by neurons and oligodendrocytes in the spinal cord. PTPα and F3 form a membrane-spanning co-receptor complex.[7] Given that both neurons and oligodendrocytes express F3,[5,11] we investigated whether these two cell types could also express PTPα. Double-immunofluorescence (IF) labeling was performed on cross sections (**Fig. 1A**; a–d) and longitudinal sections (**Fig. 1A**; e and f) of cervical segments of the spinal cord from adult wild-type mice using PTPα antibody (green; **Fig. 1A**; a–f) and antibodies to markers for neurons (MAP2, red; **Fig. 1A**; a and b), oligodendrocytes (CNPase, red; **Fig. 1A**; c and d), and myelinated fibers (NF200, red; **Fig. 1A**; e and f). IF showed that PTPα was mainly expressed by neurons (**Fig. 1A**; a and b)

*Correspondence to: Zhi-Cheng Xiao; Email: zhicheng.xiao@monash.edu
Submitted: 04/01/13; Revised: 06/14/13; Accepted: 07/08/13
http://dx.doi.org/10.4161/cam.25652

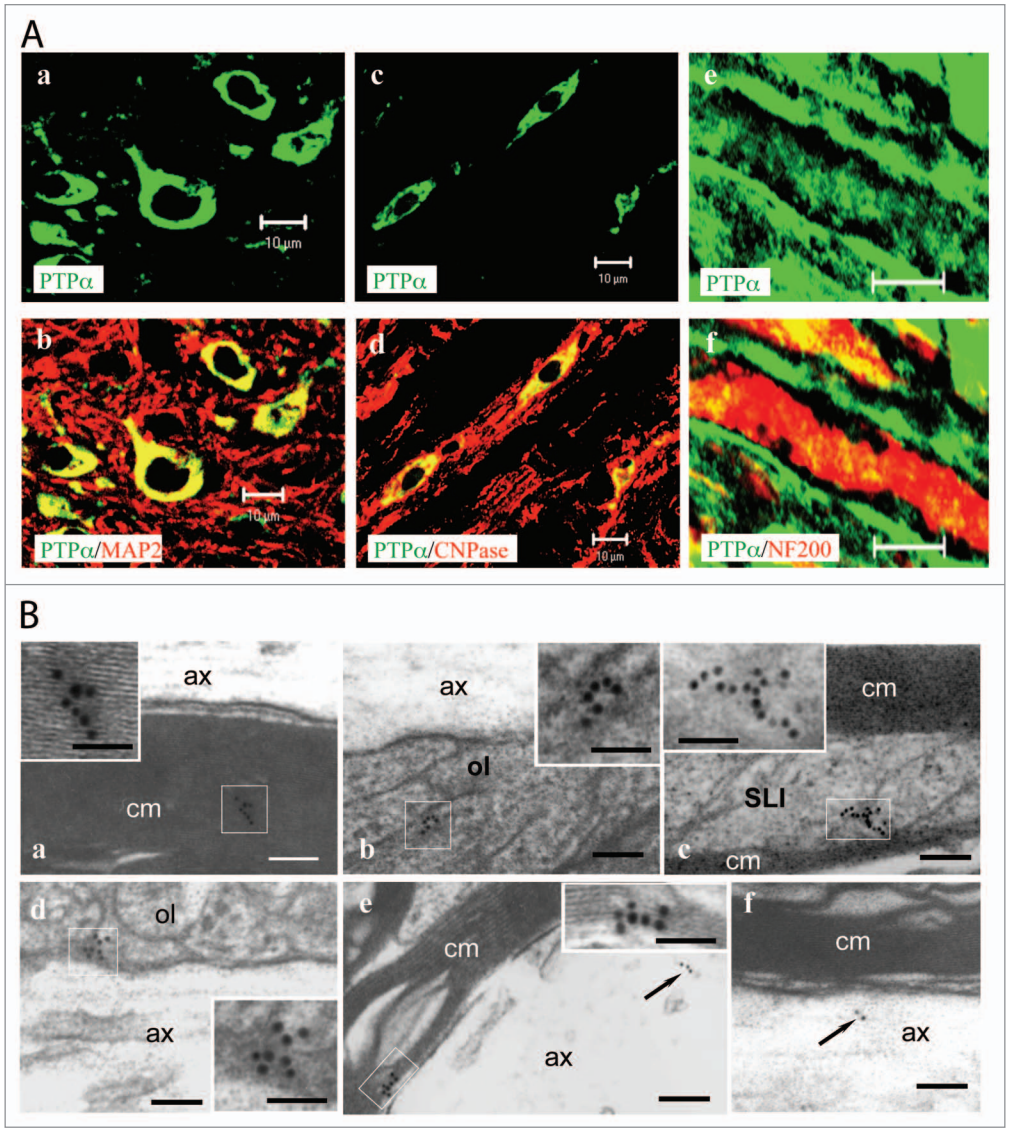

Figure 1. PTPα is expressed by both neurons and oligodendrocytes. (**A**; a–d) Cryosections of spinal cord cervical segment from adult WT mice (a–f) were double-immunolabeled for PTPα (green) and MAP2 (a and b) or CNPase (red; c and d), respectively. The overlapping (yellow in b and d) revealed that neurons (a and b) and oligodendrocytes (c and d) were positive for PTPα. Longitudinal cryosections of the spinal cords from WT mice were double-immunolabeled for PTPα (green) and NF-200 (red; e and f). PTPα was shown to distribute uniformly along the NF-200-labeled axons. Bars: 10 μm for a–d; 40 μm for e and f. (**B**) Following immunogold labeling of PTPα in ultra-thin sections, particles were detected on the compact myelin sheaths (a and e), within paranodal loops (b), Schmidt Lanterman incisures (c), the tips of paranodal loops (d) as well as the axons (e and f, arrows). The boxed areas of a–e at higher magnification are shown in the insets. ax, axon; cm, compact myelin; ol, oligodendrocyte loop; SLI, Schmidt Lanterman incisure. Bars: 100 nm for a–f; 50 nm for the insets.

and oligodendrocytes (**Fig. 1A**; c and d) and evenly distributed along myelinated axons (**Fig. 1A**; e and f). Moreover, the subcellular location of PTPα was investigated by immunoelectron-microscopy. Consistently, PTPα immunoreactivity was high in the compact myelin sheath (**Fig. 1B**; a), oligodendrocyte loops (**Fig. 1B**; b), Schmidt-Lanterman incisures (**Fig. 1B**; c), axoglial junctions at paranodes (**Fig. 1B**; d), and inner myelin sheaths at internodes (**Fig. 1B**; e). PTPα immunoreactivity was also present in myelinated axons (**Fig. 1B**; e and f). Altogether, these observations demonstrate that PTPα is mainly expressed by neurons and oligodendrocytes, suggesting that PTPα may play a role in the spinal cord myelination.

Abnormal myelination appears in the spinal cord of PTPα mutant mice. To ascertain whether the myelin structure is compromised in PTPα-null (KO) mice, we analyzed myelin profiles in the lateral funiculus of the cervical spinal cord of both PTPα KO and wild-type (WT) mice at post-natal day 60 (P60) using electromicroscopy (EM). Compared with WT littermates (**Fig. 2A**; a), abnormal CNS myelin sheaths in the mutant mice were significantly increased (**Fig. 2A**; b to e; WT: 1.089 ± 0.53%; KO: 3.745 ± 1.14%; $P < 0.005$), including vacuolations that contain myelin debris in the innermost myelin layer (**Fig. 2A**; c), and multiwheel myelin sheaths (**Fig. 2A**; d). Moreover, an obvious augmentation was found in the number

of myelin sheaths in the mutants (**Fig. 2B**; a and b) compared with WT (**Fig. 2B**; c).

To investigate the role of PTPα in myelination, EM analyses of lateral sections of the cervical spinal cord showed that in adult KO mice, myelin sheaths were noticeably thicker than in WT littermates (**Fig. 2B**; a to c). Myelination was then quantitatively examined by measuring the *g* ratio (ratio of axon diameter to diameter of myelinated fiber). In the KO animals, the *g* ratio (0.772 ± 0.003; mean ± SEM) was significantly lower than in WT animals (0.784 ± 0.002; **Fig. 2B**; d). Consistently, quantification of myelinated axons at this developmental stage showed that in KO mice, 81.14% axons were myelinated, which was significantly higher than in WT animals (71.81%; $P < 0.005$; **Fig. 2B**; e). These observations corroborate that PTPα plays a role in modulating myelination.

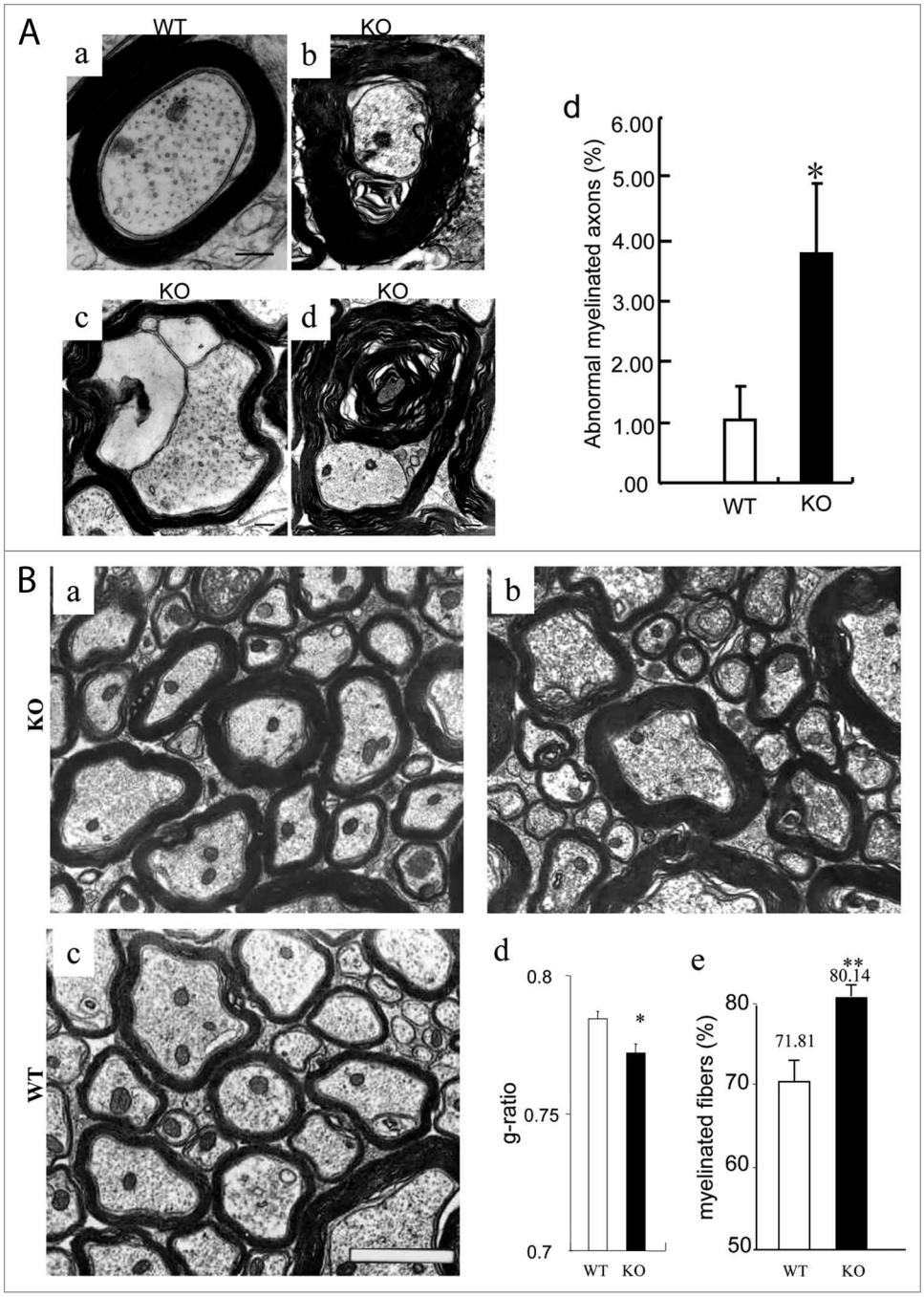

Figure 2. Abnormal myelination in PTPα KO mice. (**A**) Abnormal appearance of the myelin sheathes in PTPα-deficient mice (c and d). As compared with WT (a), the thicker myelin sheathes (b), the vacuolar (c), multiwheel (d) structures were noted in the mutants. Numbers of abnormal myelination were quantified in adult KO animals vs. WT littermates (e). Scale bars: 2 μm. (**B**) EM analyses of cross-sections of the lateral funiculus of the cervical spinal cord of P60 PTPα KO (a and b) and WT littermates (c). It was revealed that the *g* ratio significantly decreased (d) and more axons were myelinated in KO mice at this adult stage (e). Scale bars: 2 μm. *: $P < 0.05$; **: $P < 0.001$.

Formation of transverse bands begins earlier in PTPα mutant mice. Both Caspr and F3 are constituents of the transverse band, a hallmark of the mature paranodal junction.[4] To explore the role of PTPα in axoglial interaction at the paranodal region, we investigated transverse band formation at paranodes on longitudinal sections of myelinated fibers in the spinal cord. In WT mice, EM showed that transverse bands were barely detectable at P15 (**Fig. 3A**; a), and became distinct by P18 (**Fig. 3A**; b). Interestingly, these bands were readily observed as early as P13 (**Fig. 3A**; c) and became prominent by P15 (**Fig. 3A**; d) in KO mice. We then counted the number of transverse bands at the paranode, which showed a significant increase in P15 KO animals as compared with P15 WT littermates (**Fig. 3A**; e). To further explore the role of PTPα in paranodal architecture, we performed immunofluorescent double labeling of Na^+ channel (pan, red) and Caspr (green) on the longitudinal sections of lateral cervical spinal cord in both WT littermates and PTPα mutants. IF showed that the length of Na^+ labeling at the nodes was normal, while Caspr labeling at the paranodes was significantly shortened in the KO mice as compared with WT ($P < 0.001$; **Fig. 3B**). These observations suggest that the ablation of PTPα leads to the precocious formation of transverse bands, and affects the formation of the paranodal apparatus in the spinal cord of the mutant mice.

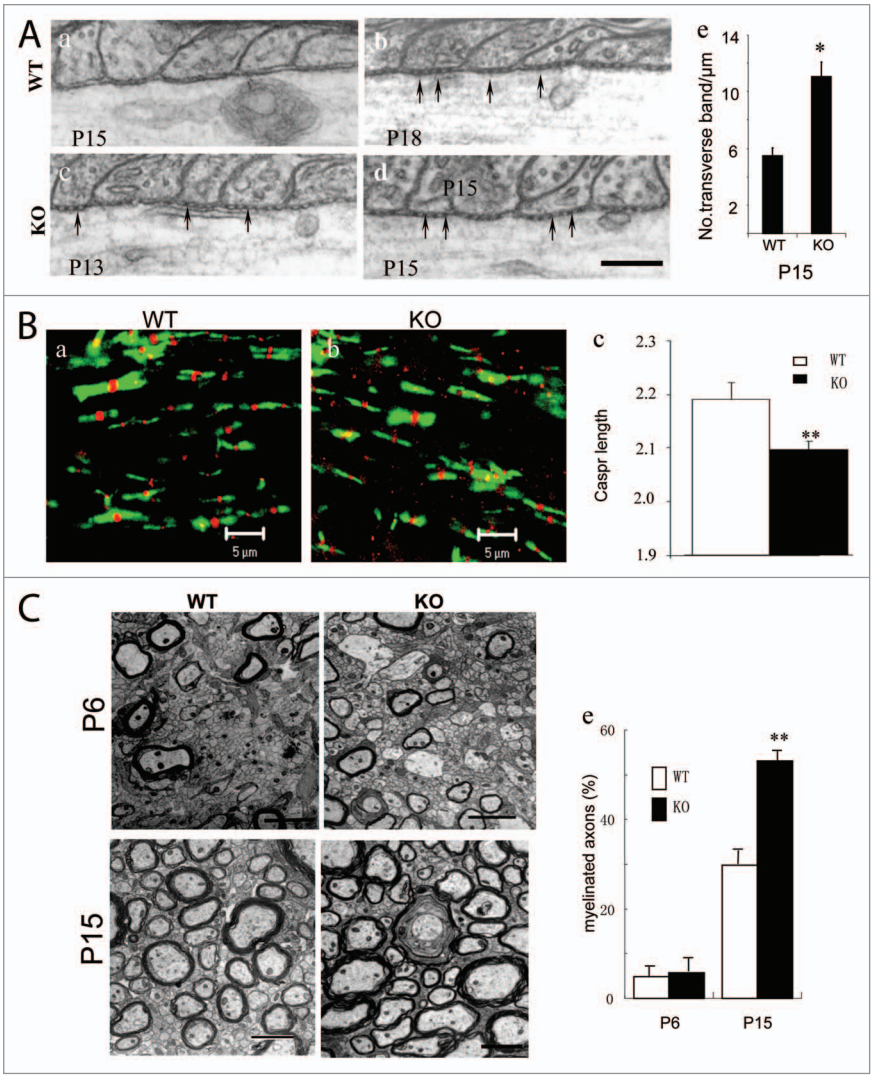

Figure 3. Myelination is accelerated in the CNS of PTPα KO mice. (**A**) Transverse bands appeared earlier in the spinal cord of PTPα mutant mice. EM analyses of paranodal axoglial junctions showed that on longitudinal sections of spinal cord from P15 WTs, transverse bands were hardly to be observed (a). They were obviously present at P18 instead (b; arrows). However, in mutants at P15 (d; arrows) and even as early as at P13 (c; arrows), transverse bands were clearly observed. Numbers of transverse bands at the paranode were quantified in P15 KO animals vs. WT littermates (e). Bar: 200 nm. *: $P < 0.05$. (**B**) Immunofluorescent double labeling of Na^+ channel (red) and Caspr (green) on the longitudinal sections of lateral cervical spinal cord in both WT littermates (a) and PTPα mutants (b). As marked by Caspr antibodies, the paranodal labelings were shorter in PTPα KO (c) than in WT mice. **: $P < 0.001$. (**C**) EM analyses of cross-sections of lateral funiculus of cervical spinal cords from both PTPα mutants and the WT littermates at P6 and P15, respectively. At P6, the profiles of myelination were similar in both wild-type (a and e) and PTPα mutant (c and e) mice. However, at P15, the quantification results revealed that the myelinated fibers were increased in PTPα mutant mice (d and e), when compared with the wild-type littermates (b and e). Bars: 2 μm. **: $P < 0.001$.

Myelination progresses faster in the spinal cord of the PTPα mutant mice. Our observations of the early formation of transverse bands and the increased number of oligodendroglial loops at paranodal regions in PTPα-deficient mice suggested that early and faster myelination might be induced in the absence of PTPα in the spinal cord. To directly investigate the role of PTPα in myelination, EM was performed in P6 (**Fig. 3C**; a and c) and P15 (**Fig. 3C**; b and d) PTPα WT (**Fig. 3C**; a and b) and KO (**Fig. 3C**; c and d) mice. Quantification of myelinated fibers in cross sections of the lateral funiculus of the cervical spinal cord showed no significant difference between the percentages of myelinated fibers in the KO (5.72 ± 3.10%) and WT mice (5.01 ± 2.03%; **Fig. 3C**; e) at P6. Notably, in P15 KO mice, around twice as many fibers were myelinated as in WT littermates (53.00 ± 1.05% vs. 29.73+2.11%, respectively; $P < 0.005$; **Fig. 3C**; e). Consistent with the precocious formation of transverse bands at paranodes, these observations indicate that myelination in PTPα KO mice progresses faster during early spinal cord development.

Paranodal length is shortened in the spinal cord of the PTPα mutant mice. To further confirm the altered paranodal architecture in the spinal cord of the mutant mice, EM analysis was performed. The paranodal region was demarcated as indicated (**Fig. 4A**; a and b; the region within the two vertical bars). As observed, the length of nodes was comparable between mutant and WT mice (**Fig. 4A**; c). In agreement with the IF observation, the length of paranodes in the mutants (3.00 ± 0.09 μm; mean ± SD) was significantly shortened as compared with WT (3.59 ± 0.09 μm; $P < 0.001$) (**Fig. 4A**; a to c). These results demonstrate that PTPα regulates the formation of axoglial junctions during myelination.

Non-landed oligodendroglial loops are increased in the spinal cord of the PTPα mutant mice. Axoglial contact at the paranode has been proposed to serve as an anchor point between axons and myelin loops and also as an initial site for myelination.[3,5] To explore the role of PTPα in myelination, we examined the compactness of myelin loops at the paranode by quantifying the number of loops in a given length. In PTPα KO mice, there were more myelin loops per micrometer than in WT mice (**Fig. 4A**; d), demonstrating that myelin sheaths are more compact in KO mice. Since myelin loops comprised landed and non-landed loops, we further quantified these two types of loops in each pananode. This revealed that the number of total oligodendroglial loops per paranode was significantly increased in KO vs. WT mice, mainly due to a significant increase in non-landed loops (**Fig. 4A**; e). These results further confirm that the ablation of PTPα leads to abnormal myelination in the mutant mice.

More small axons are myelinated in PTPα mutant mice. Given that myelin-related protein expression is not globally

upregulated in the spinal cord of PTPα KO mice (not shown), we grouped the myelinated and unmyelinated fibers by axon diameter (< 1.0 μm; 1.0~1.5 μm; 1.5~2.0 μm; 2.0~3.0 μm; > 3.0 μm) to thoroughly characterize the role of PTPα in determining myelin formation and myelin thickness. We found that the percentage of myelinated fibers with an axonal diameter less than 1.0 μm was higher in the spinal cord of the adult PTPα KO than in WT mice (**Fig. 4B**; a). Consistently, the *g* ratio showed that abnormal myelination in PTPα KO mice was more evident in small axons (< 1.5 μm; $P < 0.005$) than in large ones (> 1.5 μm) (**Fig. 4B**; b). Thus, the observation that mutant mice show corresponding decreases in the percentages of larger (> 1.0 μm) myelinated axons is consistent with a larger portion of a given amount of myelin-related proteins being redirected to small axons, suggesting that PTPα may regulate the axon size-dependent allotment of an existing pool of myelin-related proteins.

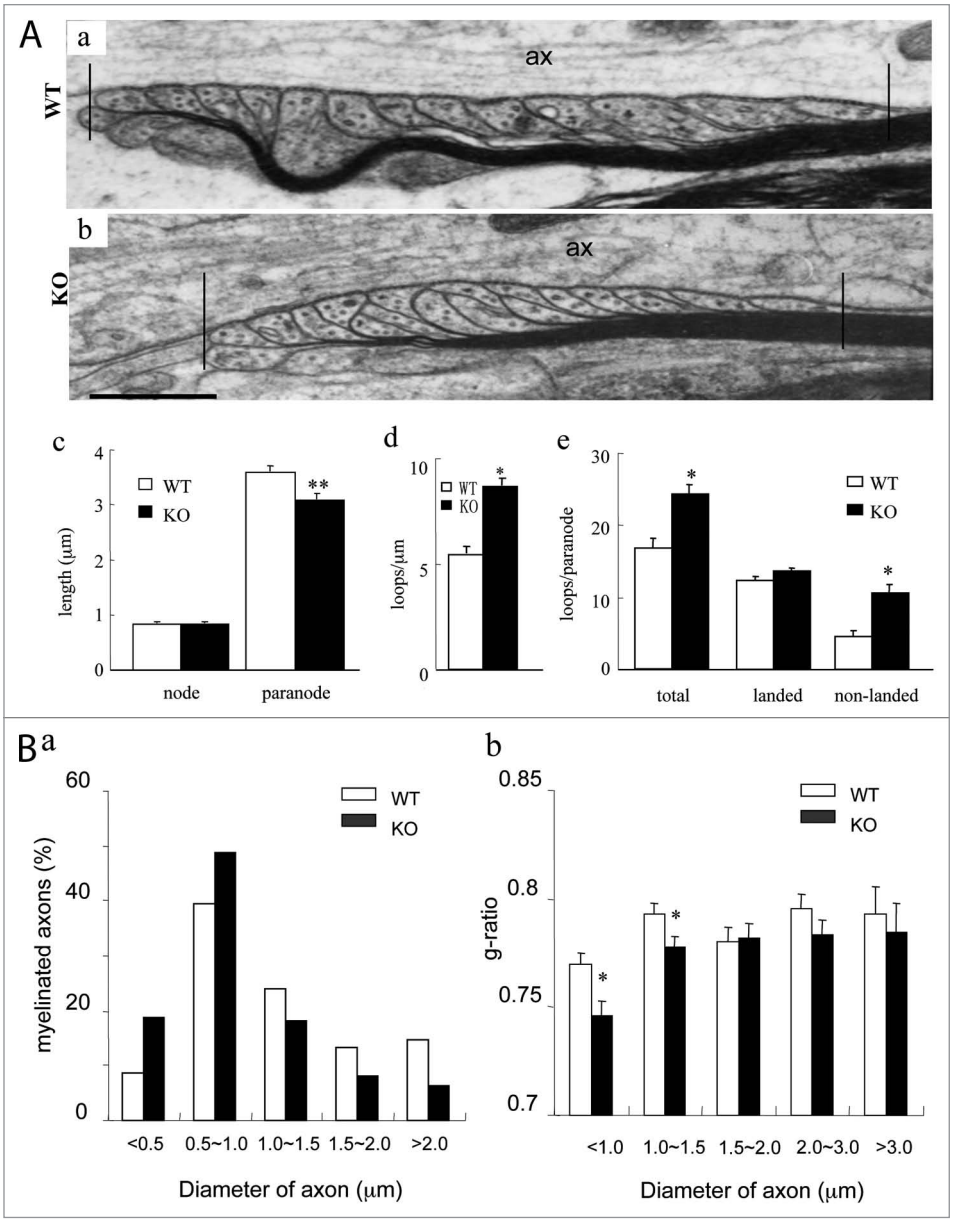

Figure 4. Paranodal apparatus and distribution of the myelin-related proteins in PTPα-deficient mice. (**A**) EM analyses revealed that the paranode, but not the node, was shortened in PTPα mutant mice (a–c); there were more myelin loops in the paranodal region of mutant mice than in WT mice (a, b, and e). The paranodal region was demarcated as shown in (a and b). Particularly, a lot more of non-landed loops appeared in mutant animals (a, b, and e). Vertical bars in (a and b) indicate the boundaries of paranode. ax, axon. Bars: 500 nm for a and b. Raw data were obtained from at least 24 paranodes in each genotype. *: $P < 0.005$; **: $P < 0.001$. (**B**) More small axons are myelinated developmentally in PTPα mutant mice. In adult animals, it was revealed that myelinated fibers (a), especially smaller myelinated fibers (b), were increased by the PTPα deletion in comparison with the WT in that more axons < 1.0 μm, but not those > 1.0 μm in diameter were myelinated in mutant mice. Values represent least three mice of each genotype. *: $P < 0.005$.

Discussion

We have found that PTPα is mainly expressed in both neurons and oligodendrocytes in the spinal cord. In PTPα-deficient mice, the formation of transverse bands at the paranodal region and myelination are accelerated during early development, which leads to abnormal myelination in the adult spinal cord. Thus, PTPα acts as a role in myelination during spinal cord development.

Axoglial interaction is precisely regulated during lineage maturation through multiple signaling pathways.[13,14] F3 is the first GPI-linked molecule identified that is located in both nodal and paranodal regions.[15,16] It forms an intracellular complex with paranodin, a single transmembrane protein[17] also termed Caspr and modulates its transfer from the endomembrane system to the axolemma.[15,18] F3 also is clustered at the paranode, a critical site of axoglial dialog for initiating myelination, from the first postnatal week.[16] PTPα interacts with F3 to form a membrane-spanning co-receptor complex, which potentially transduces extracellular signals.[7] Similar to F3, PTPα is expressed by both neuron and oligodendrocytes in the CNS. However, it distributes evenly along myelinated axons, such as compacted myelin, oligodendroglial loops, and axoglial junctions, implying that PTPα exists as a membrane-spanning complex with F3 at both nodal and paranodal regions.[7]

In PTPα KO mice, transverse bands are formed from P13 and myelinated axons are significantly increased by 20% at P15,

indicating that myelination occurs earlier in the KO animals. The early formed transverse bands accumulate axonal signaling molecules, such as F3 and Caspr, which might lead to advanced meylination in the spinal cord of PTPα mutant. Further analyses reveal that in these KO mice, myelin sheaths become thicker, myelin loops are more compact, and the non-landed oligodendrocyte loops increases, suggesting that axonal PTPα may not only regulate the integrity of the paranodal apparatus but also restrict myelination. Further observations that there is a significant increase in the number of myelinated axons at P15 and in the adult as well as a significant decrease in the *g*-ratio of adult mutant mice demonstrate that PTPα ablation leads to abnormal myelination during both early and later stages of development.

Myelination occurs in accordance with axon size, as axons with diameters less than 0.2 μm are usually unmyelinated in the CNS.[19] However, in PTPα KO mice, more small axons with diameters less than 1.5 μm are preferentially myelinated, while in the large axons the *g*-ratio did not change. Thus, the disparity may well be explained by the fact that in PTPα mutant mice, more small axons are myelinated at the cost of myelinating larger axons, that is, a larger portion of a given amount of myelin-related proteins seems to "flow" to the small axons. Given that initiating myelination is dependent on signals from the axon but is not due to the intrinsic program of oligodendrocytes,[20] it is possible that PTPα takes part in abnormal myelination in the spinal cord of PTPα KO mice. As such, in small axons, higher expression of PTPα may be responsible for reducing F3 clustering at axoglial junctions, and blocking myelination. However, perhaps because of technical limitations, we were unable to detect any difference between small and large axons in expression of PTPα and F3/contactin clustering at the paranode, and this remains to be further investigated.

The tyrosine kinase Fyn, a signaling molecule downstream of MAG, has been implicated in the initiation of myelination.[8] Hypomyelination of the optic nerve is significantly increased by ~40–50% in Fyn-deficient mice and by ~80% in MAG/Fyn-deficient mice.[21,22] PTPα is a physiological activator of Fyn as demonstrated by the 60% reduced kinase activity of Fyn in brains of PTPα-deficient mice compared with WT mice.[12] The distinct phenotypes of the respective single and double mutants suggest that there may be multiple signaling pathways involved in myelination. In support of this, it is worth noting that Fyn-knockout mice show CNS region-specific deficiencies in myelination, with spinal cord myelination appearing normal while forebrain myelination is impaired.[23] Thus, in addition to or besides activating Fyn, PTPα may negatively regulate other downstream elements that are positively involved in axonal ensheathment. Precisely how the absence of PTPα alters the balance among Fyn, Notch, and other pathways in oligodendrocytes during myelinogenesis, leading to an over-ensheathment of axons, remains to be explored.

PTPs are highly expressed in the nervous system, suggesting that they may play multiple roles during development.[24] It is also conceivable that a potential compensatory upregulation of other PTPs, such as PTPε that has been identified as a positive modulator of myelination,[25] may be related to abnormal myelination in PTPα KO mice. Taken altogether, our results demonstrate that PTPα reduces the F3 clustering along the axoglial interface and plays a role in regulating myelination in the spinal cord. These findings provide a significant insight into how to promote remyelination in demyelinated spinal cord, such as multiple sclerosis, through manipulating PTPα.

Experimental Procedures

Antibodies. Polyclonal antibodies to PTPα,[7] Caspr,[11] and monoclonal antibodies to sodium channels (PAN) (Sigma), were used. Secondary antibodies included goat anti-rabbit IgG (Amersham), goat anti-mouse IgG (Amersham), Cy3-conjugated anti-rabbit IgG (Amersham), and Cy2-conjugated anti-mouse IgG (Amersham).

Conventional electron microscopy. Postnatal day 6 (P6), P13, P15, P18, and P60 PTPα-knockout (KO)[12] and corresponding wild-type (WT) littermate mice were deeply anesthetized and transcardially perfused with Ringer's solution, followed by a fixative mixture of 2% paraformaldehyde and 3% glutaraldehyde in 0.1 M sodium phosphate buffer, pH 7.4. Cervical spinal cord was then removed, trimmed to minimize excess tissue, and immersed for 2 h in the same fixative mixture. Tissue blocks were then washed in 0.1 M sodium phosphate buffer and incubated 1 h in 2% osmium tetroxide. Blocks were washed in 0.1 M sodium phosphate buffer, dehydrated in ethanol, and infiltrated and embedded in Araldite. Semi-thin sections for light microscopy were cut using an ultramicrotome and stained with toluidine blue. Thin sections for electron microscopy were cut using an ultramicrotome, stained with uranyl acetate and lead citrate, and observed under a JEOL 1220 electron microscope.

Immunohistochemistry and immunoelectron microscopy. Adult PTPα-deficient and wild-type littermate mice were deeply anesthetized and transcardially perfused with Ringer's solution, followed by 4% paraformaldehyde in 0.1 M phosphate buffer (PB), pH 7.4. Cervical spinal cord and brainstem were harvested and post-fixed in 4% paraformaldehyde for 2 h and processed for immunohistochemistry as previously described.[26] For electron microscopy, samples from adult wild-type mice were prepared according to published protocols,[26] and examined under a JEOL 1220 electron microscope.

Quantitative analysis of EM data. The percentages of myelinated fibers were determined in cross sections of lateral funiculi of cervical spinal cords from P6, P15, and P60 PTPα KO and WT littermates. Randomly selected non-overlapping fields were photographed at a magnification of 10,000×. Myelinated and unmyelinated axons with a visible entire circumference and under upper and lateral borders on the electron micrographs were counted from at least three animals of each age and genotype. Statistical analysis of data was performed using the chi-square test.

Longitudinal sections of lateral funiculi of cervical spinal cords from P60 PTPα KO and WT littermates were employed to determine the lengths of node and paranode, as well as the number of oligodendrocyte loops. Electron micrographs were taken only of profiles of longitudinally oriented axons that displayed

at least one complete paranode at magnifications between 8,000~12,000× and scanned into digital data. The measurements were taken using a Leica Qfluoro system. Lengths of Caspr positive areas were measured using a Zeiss LSM Image Browser system. Statistical analyses of data were performed using the one-way ANOVA test under ORIGIN 5.0.

Disclosure of Potential Conflicts of Interest

No potential conflicts of interest were disclosed.

Acknowledgments

We thank Prof C.J. Pallen for providing PTPα-knockout mice and constructional discussion as well as the technique assistant from Drs BT Ang and S Ponniah. This work was supported by grants to ZC Xiao from Talent Program of Yunnan Province and The Professorial Fellowship of Monash University and to QH Ma from National Natural Science Foundation of China (31171313).

References

1. Hirano A, Dembitzer HM. Further studies on the transverse bands. J Neurocytol 1982; 11:861-6; PMID:6185646; http://dx.doi.org/10.1007/BF01148304
2. Ichimura T, Ellisman MH. Three-dimensional fine structure of cytoskeletal-membrane interactions at nodes of Ranvier. J Neurocytol 1991; 20:667-81; PMID:1719139; http://dx.doi.org/10.1007/BF01187068
3. Rosenbluth J, Liang WL, Liu Z, Guo D, Schiff R. Paranodal structural abnormalities in rat CNS myelin developing in vivo in the presence of implanted O1 hybridoma cells. J Neurocytol 1995; 24:818-24; PMID:8576711; http://dx.doi.org/10.1007/BF01179981
4. Salzer JL. Polarized domains of myelinated axons. Neuron 2003; 40:297-318; PMID:14556710; http://dx.doi.org/10.1016/S0896-6273(03)00628-7
5. Hu QD, Ang BT, Karsak M, Hu WP, Cui XY, Duka T, et al. F3/contactin acts as a functional ligand for Notch during oligodendrocyte maturation. Cell 2003; 115:163-75; PMID:14567914; http://dx.doi.org/10.1016/S0092-8674(03)00810-9
6. Pallen CJ. Protein tyrosine phosphatase alpha (PTPalpha): a Src family kinase activator and mediator of multiple biological effects. Curr Top Med Chem 2003; 3:821-35; PMID:12678847; http://dx.doi.org/10.2174/1568026033452320
7. Zeng L, D'Alessandri L, Kalousek MB, Vaughan L, Pallen CJ. Protein tyrosine phosphatase alpha (PTPalpha) and contactin form a novel neuronal receptor complex linked to the intracellular tyrosine kinase fyn. J Cell Biol 1999; 147:707-14; PMID:10562275; http://dx.doi.org/10.1083/jcb.147.4.707
8. Osterhout DJ, Wolven A, Wolf RM, Resh MD, Chao MV. Morphological differentiation of oligodendrocytes requires activation of Fyn tyrosine kinase. J Cell Biol 1999; 145:1209-18; PMID:10366594; http://dx.doi.org/10.1083/jcb.145.6.1209
9. Umemori H, Sato S, Yagi T, Aizawa S, Yamamoto T. Initial events of myelination involve Fyn tyrosine kinase signalling. Nature 1994; 367:572-6; PMID:7509042; http://dx.doi.org/10.1038/367572a0
10. Liang X, Draghi NA, Resh MD. Signaling from integrins to Fyn to Rho family GTPases regulates morphologic differentiation of oligodendrocytes. J Neurosci 2004; 24:7140-9; PMID:15306647; http://dx.doi.org/10.1523/JNEUROSCI.5319-03.2004
11. Nie DY, Zhou ZH, Ang BT, Teng FY, Xu G, Xiang T, et al. Nogo-A at CNS paranodes is a ligand of Caspr: possible regulation of K(+) channel localization. EMBO J 2003; 22:5666-78; PMID:14592966; http://dx.doi.org/10.1093/emboj/cdg570
12. Ponniah S, Wang DZ, Lim KL, Pallen CJ. Targeted disruption of the tyrosine phosphatase PTPalpha leads to constitutive downregulation of the kinases Src and Fyn. Curr Biol 1999; 9:535-8; PMID:10339428; http://dx.doi.org/10.1016/S0960-9822(99)80238-3
13. Mehler MF. Mechanisms regulating lineage diversity during mammalian cerebral cortical neurogenesis and gliogenesis. Results Probl Cell Differ 2002; 39:27-52; PMID:12357985; http://dx.doi.org/10.1007/978-3-540-46006-0_2
14. Yung SY, Gokhan S, Jurcsak J, Molero AE, Abrajano JJ, Mehler MF. Differential modulation of BMP signaling promotes the elaboration of cerebral cortical GABAergic neurons or oligodendrocytes from a common sonic hedgehog-responsive ventral forebrain progenitor species. Proc Natl Acad Sci USA 2002; 99:16273-8; PMID:12461181; http://dx.doi.org/10.1073/pnas.232586699
15. Boyle ME, Berglund EO, Murai KK, Weber L, Peles E, Ranscht B. Contactin orchestrates assembly of the septate-like junctions at the paranode in myelinated peripheral nerve. Neuron 2001; 30:385-97; PMID:11395001; http://dx.doi.org/10.1016/S0896-6273(01)00296-3
16. Kazarinova-Noyes K, Malhotra JD, McEwen DP, Mattei LN, Berglund EO, Ranscht B, et al. Contactin associates with Na+ channels and increases their functional expression. J Neurosci 2001; 21:7517-25; PMID:11567041
17. Menegoz M, Gaspar P, Le Bert M, Galvez T, Burgaya F, Palfrey C, et al. Paranodin, a glycoprotein of neuronal paranodal membranes. Neuron 1997; 19:319-31; PMID:9292722; http://dx.doi.org/10.1016/S0896-6273(00)80942-3
18. Faivre-Sarrailh C, Falk J, Pollerberg E, Schachner M, Rougon G. NrCAM, cerebellar granule cell receptor for the neuronal adhesion molecule F3, displays an actin-dependent mobility in growth cones. J Cell Sci 1999; 112:3015-27; PMID:10462518
19. Hildebrand C, Remahl S, Persson H, Bjartmar C. Myelinated nerve fibres in the CNS. Prog Neurobiol 1993; 40:319-84; PMID:8441812; http://dx.doi.org/10.1016/0301-0082(93)90015-K
20. Fanarraga ML, Griffiths IR, Zhao M, Duncan ID. Oligodendrocytes are not inherently programmed to myelinate a specific size of axon. J Comp Neurol 1998; 399:94-100; PMID:9725703; http://dx.doi.org/10.1002/(SICI)1096-9861(19980914)399:1<94::AID-CNE7>3.0.CO;2-5
21. Umemori H, Kadowaki Y, Hirosawa K, Yoshida Y, Hironaka K, Okano H, et al. Stimulation of myelin basic protein gene transcription by Fyn tyrosine kinase for myelination. J Neurosci 1999; 19:1393-7; PMID:9952416
22. Biffiger K, Bartsch S, Montag D, Aguzzi A, Schachner M, Bartsch U. Severe hypomyelination of the murine CNS in the absence of myelin-associated glycoprotein and fyn tyrosine kinase. J Neurosci 2000; 20:7430-7; PMID:11007902
23. Sperber BR, Boyle-Walsh EA, Engleka MJ, Gadue P, Peterson AC, Stein PL, et al. A unique role for Fyn in CNS myelination. J Neurosci 2001; 21:2039-47; PMID:11245687
24. Johnson KG, Van Vactor D. Receptor protein tyrosine phosphatases in nervous system development. Physiol Rev 2003; 83:1-24; PMID:12506125
25. Peretz A, Gil-Henn H, Sobko A, Shinder V, Attali B, Elson A. Hypomyelination and increased activity of voltage-gated K(+) channels in mice lacking protein tyrosine phosphatase epsilon. EMBO J 2000; 19:4036-45; PMID:10921884; http://dx.doi.org/10.1093/emboj/19.15.4036
26. Huber AB, Weinmann O, Brösamle C, Oertle T, Schwab ME. Patterns of Nogo mRNA and protein expression in the developing and adult rat and after CNS lesions. J Neurosci 2002; 22:3553-67; PMID:11978832